

# OPTIMIZED DIRECTED DECISION FREQUENCY SYNCHRONIZATION SYSTEMS IN PRESENCE OF GAUSSIAN NOISE AND OSCILLATOR PHASE NOISE

Jean-François Héland, Stéphane Bougeard  
Institut d'Electronique et de Télécommunications de Rennes (IETR)  
INSA - 20, avenue des Buttes de Coësmes  
35043 Rennes Cedex - France  
E-mail : {jean-francois.heland},{stephane.bougeard}@insa-rennes.fr

## ABSTRACT

This paper presents the performance of a directed decision frequency synchronization system associated to high order Quadrature Amplitude Modulations (QAM) in presence of Gaussian noise and local oscillator phase noise. In this study, phase noise is modelled using white Gaussian noise filtered by an analog shaping filter which has a transfer function specified by the shape of the phase noise power spectrum density. Using this model, simulation results show that an optimum trade-off between AWGN and phase noise robustness for the loop bandwidth can be determined. Furthermore, novel decision areas related to Quadrature Amplitude Modulations are determined in order to improve the performance of the carrier recovery algorithm in presence of phase noise and frequency offset.

## 1 Introduction

Recently, considerable attention has been addressed to the design of wireless systems for data rate greater than 10 Mbit/s. The larger bandwidth required to support high speed transmissions implies the choice of increasingly higher radio frequency bands, typically between 10 and 60 GHz. Nowadays, it is difficult to design low cost very high frequency local oscillators with reasonable instabilities which means that the phase noise of the local oscillator is really a technical bottleneck in the frequency range of some tens of GHz for single carrier and multi carrier systems [1][2].

A lot of broadband wireless single carrier systems have been developed at millimeter-wave frequencies between 20 and 45 GHz. Some of these cellular radio networks, referred to as Local Multipoint Distribution Service (LMDS) networks are intended to offer integrated broadband services to residential and business customers. So, with the development of these new wireless systems at high frequency, phase noise study is also sensible for high bit rate single carrier transmissions.

This paper deals with the modelling of the phase noise and the optimization of the carrier recovery of high bit rate single carrier systems in presence of phase noise. First of all, an original and efficient phase noise model based on the knowledge of its spectral density is presented. Then, the performance of a frequency synchronization system faced

with phase noise and Additive White Gaussian Noise is studied for high order modulation schemes. Thus, the optimum trade-off between AWGN and phase noise robustness for the loop bandwidth is determined. Finally, in order to increase phase noise and frequency drift tolerance, new decision areas related to Quadrature Amplitude Modulations are proposed, which leads to an efficient reduction of the acquisition time.

## 2 Phase noise modelling

The output of an oscillator affected by phase noise can be defined as

$$x(t) = (V_0 + v(t)) \sin[2\pi(f_0 + \Delta f)t + \varphi(t)] \quad (1)$$

where  $f_0$  and  $V_0$  are respectively the nominal frequency and the nominal signal amplitude.  $\Delta f$  represents the frequency drift,  $v(t)$  the amplitude fluctuation and  $\varphi(t)$  the random zero mean phase noise process characterised by its power spectral density  $S_\varphi(f)$  or its spectral purity  $L(f)$ , which is given by oscillator manufacturers. In this study, we neglect the frequency drift and the amplitude fluctuation.

In [3], it has been demonstrated that the relationship between  $L(f)$  and  $S_\varphi(f)$  is given by  $L(f) \simeq \frac{1}{2}S_\varphi(f)$  provided that  $\int_{-\infty}^{+\infty} S_\varphi(f) df \ll 1 \text{ rad}^2$ . In this study, phase noise is modelled using white Gaussian noise filtered by an analog shaping filter which has a transfer function  $H(f)$  specified by the shape of the power spectrum density according to the relation  $|H(f)| = \sqrt{S_\varphi(f)}$ . It provides a useful simulation tool which is subsequently used to take into account frequency sources impairments for the optimization of the transmission systems.

## 3 The considered carrier recovery system

In order to eliminate the frequency offset between the carrier oscillators at the transmitter and the receiver, a phase locked local oscillator can be implemented for Intermediate Frequency (IF) to baseband conversion. The considered carrier synchronization system in this study is a Decision Directed derived from the Maximum-Likelihood criterion with FeedBack and preliminarily recovered Timing (DDMLFBT) [4], [5], which is depicted in Fig. 1. This system is made up of a phase detector, a loop filter and an integrator. The phase

detector aims to provide a representative information of the phase error  $\phi(k) = \theta(k) - \hat{\theta}(k)$  between the estimated symbol  $\hat{d}(k)$  and the phase corrected sample  $w(k) = r(k) e^{-j\hat{\theta}(k)}$  where  $r(k)$  is a received sample impaired by the phase error  $\theta(k)$ . Then, this information is filtered and integrated within the loop in order to update the phase correction  $\hat{\theta}(k)$ .

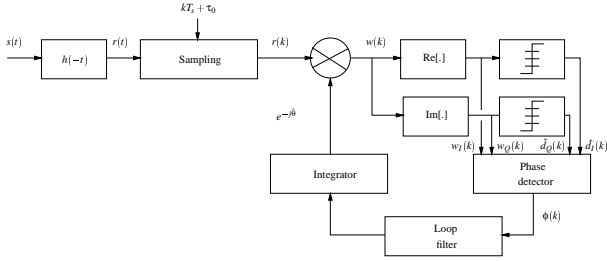


Fig. 1: DDMLFBT structure for carrier recovery

### 3.1 The phase detector

The phase error detector can be entirely defined by its characteristic  $\varepsilon[\phi(k)]$  resulting from the ML criterion application. A study on the phase detector properties carried out in [5] leads us to opt for the following characteristic

$$\varepsilon[\phi(k)] = \text{Im} [\text{csgn} [w^*(k)] [w(k) - \hat{d}(k)]] \quad (2)$$

where  $\text{csgn}(x) = \text{sgn}[\text{Re}[x]] + j\text{sgn}[\text{Im}[x]]$ .

This phase detector combined with Quadratic Amplitude Modulations provides a  $\frac{\pi}{2}$  periodic characteristic. To clear up the phase ambiguity, a differential encoding of the two most significant bits has been implemented. The size of the linear response and the slope  $K_d$  at the origin become smaller with decreasing  $E_s/N_0$ . Moreover, the values of these two parameters are all the more reduced as the order of the modulation is high. Thus, the range of representative informations  $\varepsilon(\phi)/K_d$  delivered by the phase detector decreases for low signal-to-noise ratio and high order QAM.

### 3.2 The loop characterization

A second order looped structure is used. The loop stability is achieved using the damping factor  $\zeta = 0.707$ . Furthermore, the normalized loop bandwidth is defined by the product  $B_l \cdot T_s$  with

$$B_l \cdot T_s = \frac{1}{2} \int_{-\infty}^{+\infty} |Q(f)|^2 df \quad (3)$$

where  $T_s$  is the symbol duration and  $Q(f)$  is the closed loop transfer function. The normalized loop bandwidth determines the acquisition time and the noise of the estimated phase.

## 4 Tracking performance of the DDMLFBT synchronization system

The simulated system uses squared QAM with differential encoding of the two most significant bits. The symbol rate is equal to  $F_s = 1/T_s = 6.8$  MS/s. In the receiver, the low cost local oscillator is affected by the phase noise, the spectral purity  $L(f)$  of which is described in Table 1. This phase noise is modelled using the method presented in section 2.

L(f)	Frequency offset f
-30 dBc/Hz	100 Hz
-51 dBc/Hz	1 kHz
-77 dBc/Hz	10 kHz
-95 dBc/Hz	100 kHz

Table 1: Spectral purity of a 10 GHz Local Oscillator

In this section, the tracking performance of the DDMLFBT synchronization system combined to Quadrature Amplitude Modulations is presented over a theoretical Gaussian channel.

### 4.1 Performance of the system

In order to determine the optimum value of the normalized loop bandwidth  $B_l \cdot T_s$  in presence of phase noise and additive white Gaussian noise, the performance of the systems using the DDMLFBT algorithm has been measured versus  $B_l \cdot T_s$ . The BER obtained for 16-QAM is plotted in Fig. 2 versus various signal-to-noise ratio  $E_s/N_0$ .

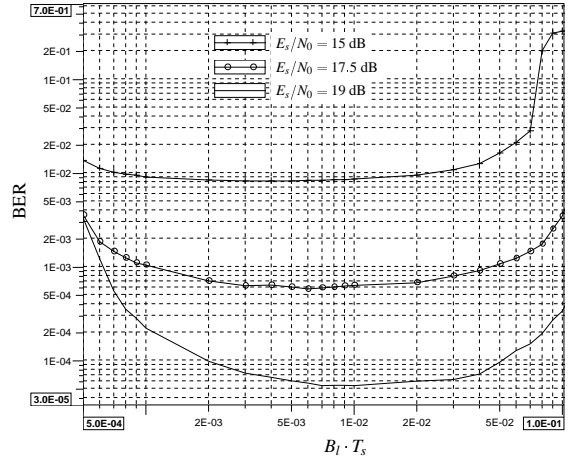


Fig. 2: Simulated BER versus  $B_l \cdot T_s$  for 16-QAM with various SNR

The phase-locked loop gets rid of the phase noise components which fall within the loop bandwidth  $B_l$ . However, with high  $B_l$  values, Gaussian additive noise and self-noise contributions cause performance degradation. So, the BER lower limits denote the range of optimum normalized loop bandwidth values. Furthermore, results obtained for 64-QAM also bring to the fore that the more complex the modulation is, the less large the range of optimum  $B_l \cdot T_s$  values

is. Thus, it is all the more necessary to choose accurately  $B_I$  since the constellation is of a high order.

## 4.2 The phase jitter

For the tracking mode, the performance of the synchronization loop can also be defined by the phase jitter  $\sigma^2(\phi)$ , also named residual variance of the phase error. The phase jitter results from the phase noise of the local oscillator as well as the additive white Gaussian noise. Each of these two noises contributes to phase jitter in different proportions related to the choice of the loop bandwidth value. The phase jitter  $\sigma_\phi^2(\phi)$  induced by the presence of phase noise with a power spectral density  $S_\phi(f)$  at the input of the phase locked loop is given by

$$\sigma_\phi^2(\phi) = \int_{-\frac{1}{2}}^{+\frac{1}{2}} |1 - Q(fT_s)|^2 \cdot S_\phi(fT_s) d(fT_s) \quad (4)$$

where  $Q(f)$  is the closed loop transfer function of the synchronization system. On the other hand, the Cramer-Rao bound gives a lower limit of the phase jitter  $\sigma_n^2(\phi)$  resulting from an additive white Gaussian noise. It can be expressed as

$$\sigma_n^2(\phi) \geq B_I \cdot T_s \frac{N_0}{E_s} \quad (5)$$

Then, the resulting phase jitter  $\sigma^2(\phi)$  in presence of phase noise and additive Gaussian noise is defined as the sum of these two contributions

$$\sigma^2(\phi) = \sigma_\phi^2(\phi) + \sigma_n^2(\phi) \quad (6)$$

Fig. 3 shows the resulting phase jitter for a 16-QAM system in presence of the phase noise described in Table 1 and with  $E_s/N_0 = 19$  dB. The theoretical Cramer-Rao bound is given as a reference curve and the phase jitter is measured for three different symbol rates  $F_s = 1/T_s$ . These results confirm the relations (4) to (6) and reflect the greatest phase noise sensitivity of the low symbol rate systems.

## 5 Optimization of the DDMLFBT synchronization system

In this section, it is shown that the DDMLFBT combined with Quadrature Amplitude Modulations can be optimized in acquisition mode in order to improve the acquisition performance in presence of additive white Gaussian noise, phase noise and frequency offset. However, the optimizations presented for 16-QAM can be applied to any higher order Quadrature Amplitude Modulations.

### 5.1 Modifications of the decision boundary lines

Classically, the estimated symbols  $\hat{d}(k)$  used by the phase detector are delivered by a decision module based on the boundary lines  $L_B$  of the 16-QAM constellation  $C_{16}$  represented in Fig. 4. In absence of additive white Gaussian noise, the estimated symbols reliability is directly linked to

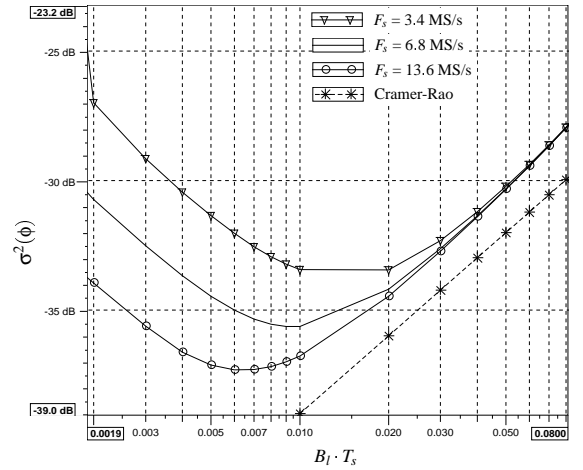


Fig. 3: Simulated residual jitter variance for 16-QAM with various symbol rates and  $E_s/N_0 = 19$  dB

the phase error sensitivity of the constellation  $C_{16}$ . The positive and negative tolerances of the four symbols of the first 16-QAM quadrant, represented in Fig. 4, are given in Table 2 where  $a = 1/\sqrt{10}$  is the energy normalization factor.

Symbols	positive tolerance	negative tolerance
(+a, +a)	+ 45 deg	- 45 deg
(+3a, +a)	+ 21.3 deg	- 18.4 deg
(+a, +3a)	+ 18.4 deg	- 21.3 deg
(+3a, +3a)	+ 16.9 deg	- 16.9 deg

Table 2: Phase error sensitivity of the 16-QAM symbols

Without noise, the size of the linear response of the phase detector can clearly be defined as equal to the lowest phase error tolerance of the external symbol (+3a, +3a). Then, the information  $\varepsilon(\phi)$  delivered at the output of the phase detector will not be representative of the phase errors which are superior to 16.9 deg. Indeed, the classical boundary lines  $L_B$ , represented in dashed lines in Fig. 4, are optimized versus the additive white Gaussian noise and they are not well adapted in presence of phase errors. In order to improve the acquisition performance, it is necessary to modify them. The geometrical representation of the modified boundary lines  $L_{BM}$ , represented in solid lines, is based on a compromise between the phase error tolerance and the additive white Gaussian noise sensitivity.

The new decision areas result from the shifting of a set of symbols along the arc of a circle in presence of phase errors. In Fig. 4, the circles centered on the four 16-QAM symbols have the radius  $r = \sigma$  and  $r = 2\sigma$  where  $\sigma$  is the standard deviation of the additive white Gaussian noise. The probability to find a symbol affected by the AWGN in a circle with a radius  $r = \sigma$  is about 90%. The general idea consists in modifying the decision boundaries in order to maximize the phase error tolerance for all the symbols included in the circle with the radius  $r = \sigma$  or with the radius  $r = 2\sigma$  when it is

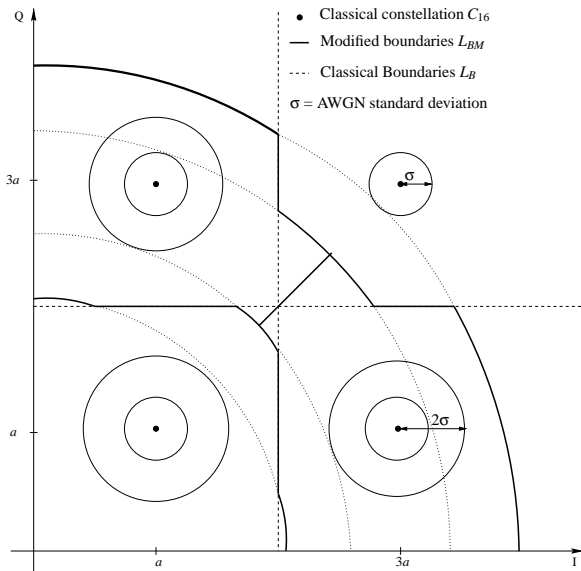


**Fig. 4:** Modified decision areas for 16-QAM; representation of the first quadrant

possible.

## 5.2 Acquisition performance of the optimized DDMLFBT system

In Fig. 5, the characteristic  $(C_{16}, L_B)$  of the detector based on the classical decisions  $\hat{d}(k)$  and the characteristic  $(C_{16}, L_{BM})$  of the detector using the optimized decisions  $\hat{d}_M(k)$  are compared for  $E_s/N_0 = 19$  dB. An increase in the size of the linear response is obtained for the optimized detector ( $3 \text{ rad}$  or  $17.2 \text{ deg}$ ), compared to the classical detector ( $2 \text{ rad}$  or  $11.5 \text{ deg}$ ). Then, the range of representative informations about the phase errors delivered by the phase detector is increased by 50%.

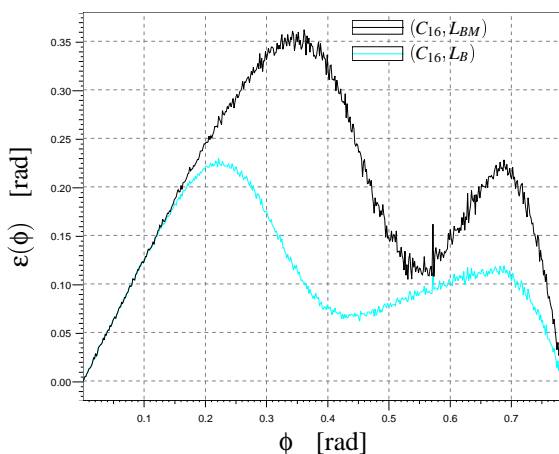


**Fig. 5:** Phase detector responses for 16-QAM using classical  $(L_B)$  and modified  $(L_{BM})$  decision areas with  $E_s/N_0 = 19$  dB

The acquisition performance of this optimized DDMLFBT

synchronisation system has been measured in presence of a frequency offset  $\Delta f_0 = 134$  kHz with  $E_s/N_0 = 19$  dB. Some acquisition times are given in Table 3 versus various normalized loop bandwidth values.

Decision module	$B_l \cdot T_s = 5 \cdot 10^{-3}$	$B_l \cdot T_s = 5 \cdot 10^{-2}$
$(C_{16}, L_B)$	$745000 T_s$	$360 T_s$
$(C_{16}, L_{BM})$	<b><math>162000 T_s</math></b>	<b><math>136 T_s</math></b>

Table 3: Acquisition times of the classical and the optimized DDMLFBT systems with  $\Delta f_0 = 134$  kHz

The optimized decision boundary lines allow to achieve acquisition time divided by about 2.5 with  $B_l \cdot T_s = 5 \cdot 10^{-2}$  and by about 4.5 with  $B_l \cdot T_s = 5 \cdot 10^{-3}$ .

## 6 Conclusion

First of all, an original phase noise model has been used to measure the performance degradations of a PLL induced by phase noise and the simulation results prove that it is possible and essential - mainly for high order modulations - to determine an optimum trade-off for the loop bandwidth. Furthermore, novel decision areas for high order QAM in presence of AWGN and phase errors have been proposed in order to improve the acquisition performance of the Decision Directed synchronisation system. Concerning these new decision areas, a patent application has been filed and it can be applied to any single carrier and multi-carrier receivers to improve the performance in presence of phase shifts [6].

Acknowledgments : The authors would like to thank FT R&D/DMR/DDH which supports and contributes to this study.

## 7 References

- [1] L. Tomba, "On the effect of Wiener phase noise in OFDM systems", *IEEE Transactions on communications*, vol. 46, no. 5, pp. 580-583, May 1998.
- [2] T. Pollet, M. Van Bladel, M. Moeneclaey, "BER sensitivity of OFDM systems to carrier frequency offset and Wiener phase noise", *IEEE Transactions of Communications*, vol. 43, no. 2/3/4, pp. 191-193, Feb./Mar./April 1995.
- [3] F. Daffara, "Model of tuner phase noise in digital simulation", *Technical report*, Philips France, dTTb/WP3.3/LEP/31, Oct. 1993
- [4] H. Meyr, M. Moeneclaey, S. A. Fechtel, *Digital communication receivers - synchronization, channel estimation and signal processing*, Wiley series in telecommunications and signal processing.
- [5] D. Mottier, "Association des fonctions d'égalisation, de synchronisation et de décodage de canal pour les transmissions numériques à grande efficacité spectrale", *Ph. D. Thesis*, INSA-Rennes, Nov. 1998.
- [6] S. Bougeard, J.F. Héland, S. Siaud, "Procédé de démodulation et de modulation d'un signal tenant compte de l'effet d'erreurs de phase, récepteur, système et signal correspondants", *Patent pending*, FR 01 06411, May 2001.